# We are IntechOpen, the world's leading publisher of Open Access books Built by scientists, for scientists

6,900
Open access books available

185,000
International authors and editors

200M
Downloads

Our authors are among the

154
Countries delivered to

TOP 1%
most cited scientists

12.2%
Contributors from top 500 universities


WEB OF SCIENCE™

Selection of our books indexed in the Book Citation Index in Web of Science™ Core Collection (BKCI)

## Interested in publishing with us?
## Contact book.department@intechopen.com

Numbers displayed above are based on latest data collected.
For more information visit www.intechopen.com

Chapter

# Dynamics of Transient Plasmas Generated by ns Laser Ablation of Memory Shape Alloys

*Stefan Andrei Irimiciuc, Norina Forna, Andrei Agop, Maricel Agop, Stefan Toma and Doriana Forna Agop*

## Abstract

Understanding the underline fundamental mechanism behind experimental and industrial technologies embodies one of the foundations of the advances and tailoring new materials. With the pulsed laser deposition being one of the key techniques for obtaining complex biocompatible materials with controllable stoichiometry, there is need for experimental and theoretical advancements towards understanding the dynamics of multi component plasmas. Here we investigate the laser ablation process on Cu-Mn-Al and Fe-Mn-Si by means of space-and time-resolved optical emission spectroscopy and fast camera imaging. In a fractal paradigm the space–time homographic transformations were correlated with the global dynamics of the ablation plasmas.

**Keywords:** shape memory alloy, laser ablation, transient plasma, optical emission spectroscopy, fractal model

## 1. Introduction

The dynamics of the ejected particles as a results of high power laser and solid matter is not a trivial problem, as it was showcased in several papers [1, 2]. The problem of complex materials, as it is the case of metallic alloys, it consists in differences in the physical properties of the composing elements. Phenomena like heterogenous melting and vaporization [3] are commonly reported for ns laser ablation, with dire consequences for applications like pulse laser deposition. Target material heterogeneity should be reflected in the dynamics of the ejected particles, which is often difficult to observe in industrial applications like laser welding, cutting, surface cleaning, but is otherwise excellent showcased in applications like LIBS or plasma spectroscopy. The amalgam of plasma entities found in a transient plasma generated by laser ablation contains ions, atoms, molecules, electron and photons. The most often used technique extensively reported by the other groups [4] or even by our group are non-invasive ones that can differentiate between the contribution of each individual component of the plasma in particular conditions even reflect the complex local and global phenomena reported in recent years. These techniques are mainly concerning the optical emission spectroscopy. Understanding laser based technologies and the interaction between high energy laser beam and metallic alloys are now relevant for a wide range of applications with fast

feedback and accurate predictions on the behavior of physical processes. The dual approach of experimental investigations and theoretical modeling has proven to be a successful method for understanding the dynamics of multi-element fluids [5, 6] or as it was showcased recently by our group for complex laser produced plasmas (LPP) [7]. The study presented in this chapter expands our previous attempts for stoichiometric transfer and plasma chemistry in the case of laser ablation of complex alloys. We discuss here the ablation of metallic particles as a result of short laser ablation interaction with ternary alloys from both an experimental and theoretical point of view. To comprehend the ablated particle dynamics we implemented optical emission spectroscopy in conjecture with ICCD fast camera imaging to record global and local information about their spatial distribution within the ablated cloud and their individual kinetic and thermal energy. From a theoretical perspective we built on our model from [7] and focused on exploring under, a fractal paradigm of motion, the effect of the plasma thermal energy (temperature) and ion physical properties (mass) on the spatial distribution of complex alloy plasmas. Usual models used to simulate the dynamics of complex systems are based on an assumption of the physical variable differentiability (e.g. density, momentum, energy, etc. [8–12] and the processes which they define. The practicality of such methods can be accepted sequentially, on space–time domains for which the differentiability still respected. However, the differential approach often fails when confronted by the reality of complex physical system (i.e. plasma plume expansion in PLD). To better represent most of the interactions at both local and global scales, it is required to introduce explicitly the scale resolution dependence. This breathes a new physical system where the variable dynamic that previously were dependent only on space and time, will now contain explicitly the dependence on the scale resolution. This can be even more abstracted and instead of using non-differential function, admittedly rather difficult to implement, just utilize different approximations of these multifractal mathematical functions derived by means of averaging at various scale resolution. A paramount consequence of this approximation is that any dynamic variable will behave as a limit of specific function families, which are non-differentiable for a null scale resolution (multifractal functions).

## 2. Laser induced plasmas on memory shape alloys

When investigating the ejected cloud of particle, the *ideal* investigation technique should be non-invasive and offer global and local information about the plasma components. Such a technique can be considered the combination of ICCD fast camera imaging and space and time resolved optical emission spectroscopy, which is used consistently by our group [7, 13, 14] and it was also validated by a significant number of papers [15, 16]. Our approach was a global - local one, meaning that the initial step was to collect the global emission (in the 300–700 nm regime) of the LPP at consecutive time-delays with respect to the laser beam. The result for a Fe-Mn-Si laser produced plasma is shown in **Figure 1**, where we present selected images during the LPP expansion in a 2 $\mu$s time lapse.

We observe that the plasma has a quasi-spherical shape and increases its volume as plasma evolves. The expansion velocity was estimated using the technique presented other previous papers [1], where it is discussed the effect of multi-element composition of the ablation process. When performing cross-section on the recorded images in axial and transversal directions, we notice different behaviors across the two directions. We also performed cross section across the main expansion axis (axial cross-section) reveals a splitting of the plasma cloud in multiple

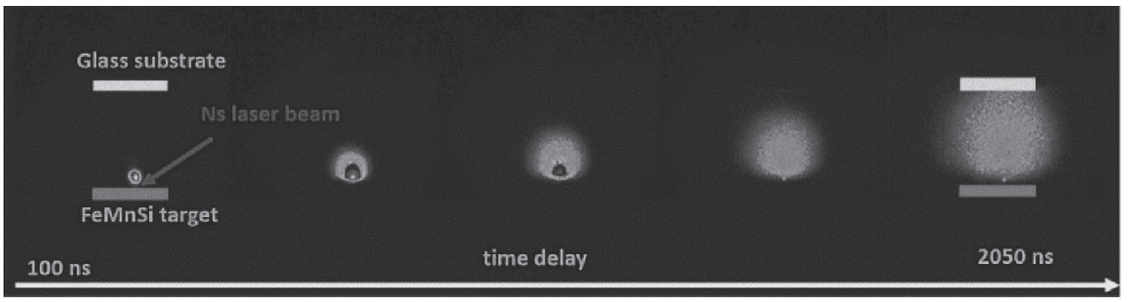


**Figure 1.**
*Global evolution of the Fe-Mn-Si LPP.*

distinct structures (two or three). Some studies report on a specific terminology for these structures, the *first one* also named the *fast one* is created by electrostatic mechanism (Cloulomb Explosion), the *second one* or *slower* structure is generated by thermal mechanisms (Explosive boiling), while the third consists of mainly clusters or nanoparticles. Their presence has beforehand been reported and extensively discussed in conjecture with the multiple ejection mechanism and their correlation with the fractality of the LPP [7, 14, 15, 17] by our group. However, our focus will not be on this third structure as the main optical signatures, seen through our experimental methods, are given by the dynamics of simpler plasma entities like atoms or ions. The velocities of the main structures were determined as follows: for the case of Cu-Mn-Al plasma – 15 km/s for the first structure and 7.4 km/s and for the second structure for the case of Fe-Mn-Si plasma - 20 km/s for the first one and 11 km/s for the second structure. The values are in good agreement with the other reports from literature [1, 18, 19]. The obtained values strongly are related to the differences of the melting points for each material and the overall mass of the cloud, with significant variance in the properties of the component directly affecting the ablation process and the subsequent evolution.

We notice a significant difference in the overall emission and shape of the LPP generated on the two alloys. The global emission is noticeably larger for the Fe-Mn-Si plasma and with less inner structuring, while for the Cu-Mn-Al the global emission is reduced and presents more pronounced structuring. These differences are induced by the energetic distribution uniformity on the excitation process as opposed to other types of interactions (i.e. ionization). Fe-Mn-Si plasma has an uniform aspect which is attributed similarities in the melting points of the composing elements, which leads to a uniform and homogeneous ablation. For the Cu-Mn-Al plasma there are significant differences between the physical properties of Al and Mn or Cu, could lead to a more heterogenous ablation process. These statements will further be verified with the space and time resolved OES. We would like to also note that, the fractality of the laser produced plasmas will also be affected by the inner energy of the plasma and its distribution on the composing entities [7, 13]. We anticipate here another type of analysis (fractal analysis) which we will further use in this study, that could offer valuable information about the laser produced plasmas.

In **Figure 2** we plotted the spatial distribution of atoms (Fe and Mn) from the Fe-Mn-Si plasma highlighting the discrepancies amongst the two elements. We would like to note that Si was not considered as the emission line intensity for its species insignificant (lower) than those of the other elements. The Fe atoms have a dual peak distribution, while the Mn one presents only a single peak distribution. This reads as Fe atoms can be excited throughout the whole plasma volume, especially at longer distance where the electron density is significantly lower. This assessment can also explain the elevated $T_{ex}$ reported earlier and it is in line with the multi-structure scenario seen by fast camera photography (ICCD fast camera

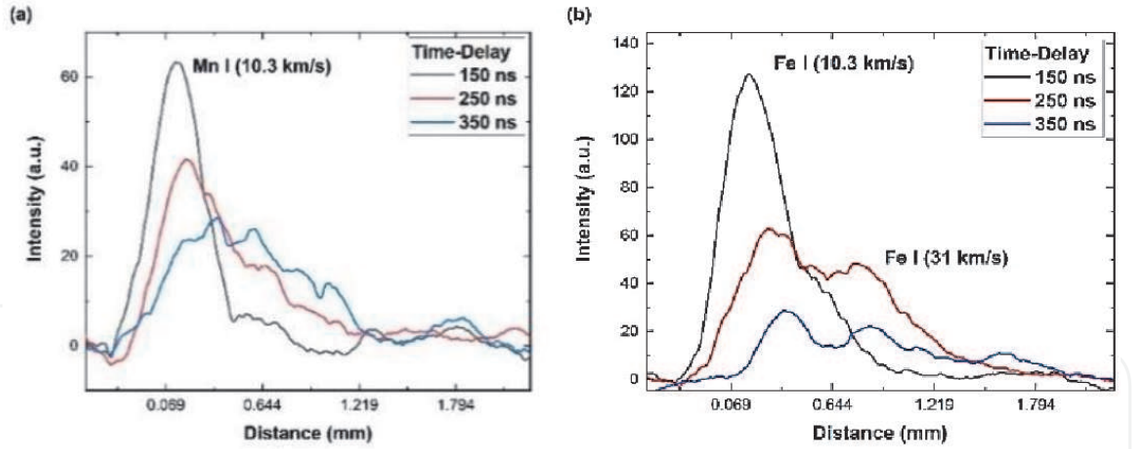


**Figure 2.**
*Axial distribution of Fe (a) and Mn (b) atomic emission at various time-delays.*

imaging). By representing the intensity maximum for individual emission line as a function of time [20], we determined the expansion velocities for the individual elements, with 31 km/s for the first peak of Fe I and 10 km/s for the second one, while for the Mn I a velocity of 18 km/s. The expansion velocity estimated for the first peak of Fe I and the Mn atoms are similar with the values of the second plasma structure, while the velocities of the second group of Fe atoms are in line with the value determined for the first plasma structure. This concludes the fact that the two-plasma structure have uniformly distributed atoms and ions amongst them with the fast structure having a slight depletion of Mn.

We can take a broader view of the discussions made in the previous paragaphs for both investigated plasmas as the laser fluence and background pressure and are (expansion conditions) identical. The results are seen in **Figure 3**-right-hand side, where we can observe for a time-delay of 150 ns the spatial distribution of Fe and Mn in the Fe-Mn-Si plasma and Cu an Al in the Cu-Mn-Al plasma, respectively. We notice that for lighter elements we obtain a narrow spatial distribution, while the *heavier* ones (Cu and Fe) have a wider distribution. These differences can be seen as a separation of the composing elements based on their physical properties. The separation was previously discussed by our group in [7, 13] where the fractality of the components played a significant role, based on that the spatial distributions of different elements are reflecting the elevated degree of fractality. Lighter elements will have a higher collision rate and thus a higher fractality degree, whereas the

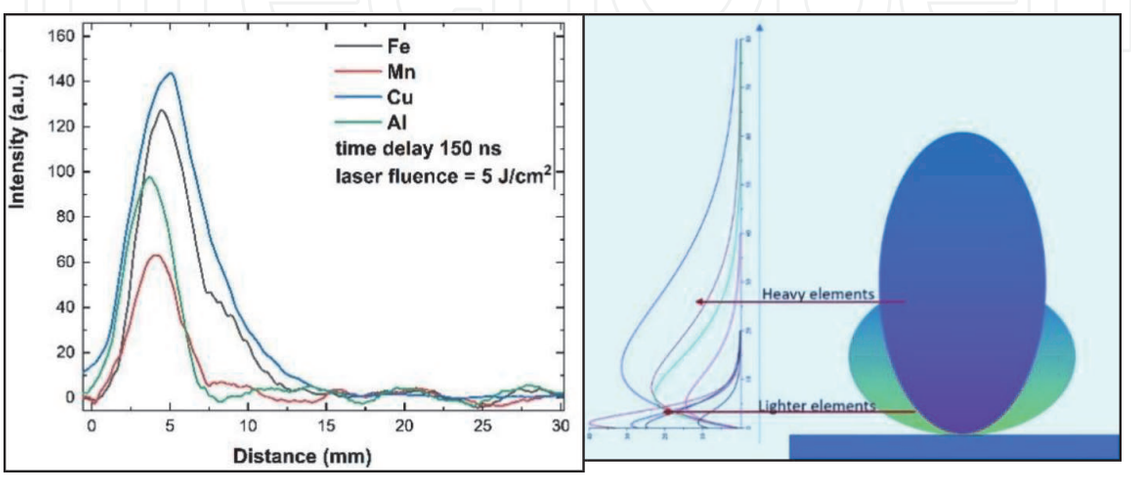


**Figure 3.**
*Axial distribution of the main elements in the alloys as seen through OES measurements at a time-delay of 150 ns (left) and a schematic representation of the particle distribution with the plasma volume (right).*

heavier ones are described by a lower fractality degree (lower collision rate). This difference in the fractality of the plasma entities will give us different spatial distributions for each element.

However, given our set-up optical configuration, lighter elements strongly scattered during expansion will appear to have a narrower distribution at relative short distances, while heavier particles will have a broader distribution most likely covering the whole plasma plume. Translating these results into the expansion of a three-dimensional plasma, low-mass elements are scattered towards the edge of the plasma plume while the high-mass ones are the building blocks the plasma core. For industrial applications like PLD, the result is of paramount importance interest as the particular volumes of the plasma plumes lack stoichiometry or uniformity. These properties could induce a non-congruent transfer of multielement material and affect the physical properties of the subsequent thin film. Furthermore, the diagnostic system used here allowed to capture the complex nature of the plasma and present some meaning behind it. We will further attempt to unravel more information about the relation between the fractality of specific elements and their spatial distribution within the plasma volume in the following section.

## 3. Theoretical modeling

The fractal analysis approach for understanding the dynamics of complex physical systems was shown over the years to provide with some of the most promising results towards understanding multiparticle flow in fluids [21, 22] or plasmas [7, 13–14, 17].

For a laser ablation plasma, the nonlinearity and the chaoticity have a dual applicability being both structural and functional, with the interactions between the so-called plasma entities (structural components like electrons, ions, atoms, photons) determine reciprocal conditioning micro–macro, local–global, individual-group, etc. In such a case, the universality of the laws describing the laser ablation plasma dynamics becomes obvious and it must be reflected by the mathematical procedures which are utilized. Basically, it makes use more and more often of the "holographic implementation" in the description of plasma dynamics. Usually, the theoretical models used to describe the ablation plasma dynamics are based on a differentiable variable assumption. Most of the notable results of the differentiable models must be understood sequentially, where the integrability and differentiability still apply. The differentiable mathematical procedures are limiting our understanding of more complex physical phenomena, such as the expansion of a laser produced plasma which implies various nonlinear behaviors, chaotic movement and self-structuring. In order to accurately describe the LPP dynamics and still remain tributary to differentiable and integral mathematics we must explicitly introduce the scale resolution. The scale resolution will be integrated in the expression of the physical variable, which describe the LPP, and implicitly in the fundamental equations, which govern these dynamics. This means that any physical variable becomes dependent on both spatial and temporal coordinates and the scale resolution. In other words, instead of using physical variables described by a nondifferentiable mathematical function, we will use different approximations of this mathematical function obtained through its averaging at various scale resolutions. As a consequence, the physical variables used to describe the LLP dynamics will act as a limit of functions family, which are non-differentiable for a null scale resolution and differentiable for non-null scale resolution.

This approach for describing LPP dynamics infers the building of novel geometric structures [23, 24] and probably new physical theories, in which the movement

laws invariant to spatio-temporal transformation, can be considered integrated on scale laws, invariant to scale resolution conversions. These geometric structures can be generated by the multifractal theory of movement in the form of Scale Relativity Theory (SRT) with a fractal dimension $D_F = 2$ [25] or in the form of SRT in an arbitrary fractal dimension [21, 22]. In both cases the "*holographic implementation*" of specific dynamics of LPP suggests a substitution of dynamics with limitations in an Euclidian space with dynamics without any restriction in a free-multifractal space. Thus, we will use only of the expansion of the plasma particles on continuous and non-differentiable curves in a multifractal space [25].

In the following we will analyze some specific dynamics of a transient plasma generated by laser ablation, therefore postulating that the plasma particles are moving on multi-fractal curves. The mathematic procedure implies the usage of the following set of multifractal hydrodynamics equations. In such a context let us consider the density current:

$$\mathfrak{J}(x,t,dt) = \rho(x,t,dt)V(x,t,dt)\sum = \frac{\sum}{\pi^{1/2}} \frac{V_0\alpha^2 + \frac{4\lambda^2(dt)^{\frac{4}{F(\sigma)}-2}}{\alpha^2}xt}{\left[\alpha^2 + \frac{4\lambda^2(dt)^{\frac{4}{F(\sigma)}-2}}{\alpha^2}t^2\right]^{3/2}} \exp\left[-\frac{(x-V_0t)^2}{\alpha^2 + \frac{4\lambda^2(dt)^{\frac{4}{F(\sigma)}-2}}{\alpha^2}t^2}\right], \tag{1}$$

where $\Sigma$ is a surface which $\mathfrak{J}$ crosses, the other parameters have the meaning given in [21, 22].

In the aforementioned conditions, $\mathfrak{J}$ is invariant with respect to the coordinates transformation group and to the scale resolutions transformation group. Since these two groups are isomorphs, between them we can unravel various isometries like: compactizations of the spatial and temporal coordinates, compactization of the scale resolutions, compactizations of the spatio-temporal coordinates and scale resolutions, etc. Following this we can perform a compactization between the temporal coordinate and the scale resolution, which is given by the relation:

$$\varepsilon = \frac{E}{m_0} = 2\lambda(dt)^{\frac{2}{F(\sigma)}-1}\upsilon, \quad \upsilon = \frac{1}{t}, \tag{2}$$

where $\varepsilon$ corresponds to the specific energy of the ablation plasma entities. Once admitted such an isometry by means of substitutions:

$$I = \frac{\mathfrak{J}\pi^{1/2}\alpha}{V_0\sum}, \quad \xi = \frac{x}{\alpha}, \quad u = \frac{\varepsilon}{\varepsilon_0}, \quad \varepsilon_0 = \frac{2\lambda V_0(dt)^{\frac{2}{F(\sigma)}-1}}{\alpha}, \quad \mu = \frac{2\lambda(dt)^{\frac{2}{F(\sigma)}-1}}{\alpha V_0}, \tag{3}$$

(1) takes the more simplified non-dimensional form:

$$I = \frac{1+\mu^2\frac{\xi}{u}}{\left(1+\mu^2\frac{\xi}{u}\right)^{3/2}} exp\left[-\frac{\left(\xi-\frac{1}{u}\right)^2}{1+\left(\frac{\mu}{u}\right)^2}\right]. \tag{4}$$

In (5.3) and (5.4) $I$ is assimilated to the normalized state intensity, $\xi$ to the normalized spatial coordinate, $\mu$ to the normalized multifractalization degree, $u$ to the normalized specific energy of the ablation plasma structures. The energy $\varepsilon$ and the reference energy $\varepsilon_0$ can be written as:

$$\varepsilon \approx \frac{T}{M}, \varepsilon_0 \approx \frac{T_0}{M_0}, \tag{5}$$

*where* $T$ and $T_0$ being the specific temperatures and $M$ and $M_0$ the specific mass, we can further note:

$$\tau = \frac{T}{T_0}, \quad \theta = \frac{M}{M_0}. \tag{6}$$

so that (5.1) becomes:

$$I = \frac{1 + \mu^2 \xi \frac{\theta}{\tau}}{\left(1 + \left(\mu \frac{\theta}{\tau}\right)^2\right)^{3/2}} \exp\left[-\frac{\left(\xi - \frac{\theta}{\tau}\right)^2}{1 + \left(\mu \frac{\theta}{\tau}\right)^2}\right]. \tag{7}$$

The fundamental transient plasmas dynamics induced by laser ablation can be corelated with a multifractal medium for which its fractality degree is echoed by the elementary processes (collision, excitations, ionization or recombination, etc. -for other details see [7, 17]). In such a context (1) defines both the normalized state intensity and it is also measure of the optical emission of each plasma structure, case for which its spatial distribution of mass type is quantified through our mathematical model and corelated with our data.

The results of our simulations are presented in **Figure 4(a,b)**. One can see that plasma entities with a fractality degree $\mu < 1$ are defined by a narrow distribution centered around small values of ξ, while for a fractality degree $\mu > 1$ the distribution is wider and is centered around values of one order of magnitude higher that the low fractality ones. Therefore, we can formulate an particular image of the plasma plume dynamics in a multifractal mathematical formalism as follows: a core of entities with low fractality and a relative low plasma temperature as well a *shell* of high energetic particles described by a higher fractality degree.

In order to perform some comparison between our results and find if they can be correlated with the classical view of the LPP we have effectuated supplementary simulations on the plasma emission distribution over the particles mass for a plasma with an overall $\mu$ factor of 5 at an arbitrary distance (ξ = 5.5). The plasma entities with a lower mass are described by a higher relative emission for a particular temperature, and with the increase of the plasma temperature the emission of high-mass elements increases as well. The obtained data is in accordance with some of our previous results from [7, 13, 17], where we correlated the plasma temperature with the plasma fractal energy. These results can have real implications for some technological applications: for low plasma excitation temperature the distribution is

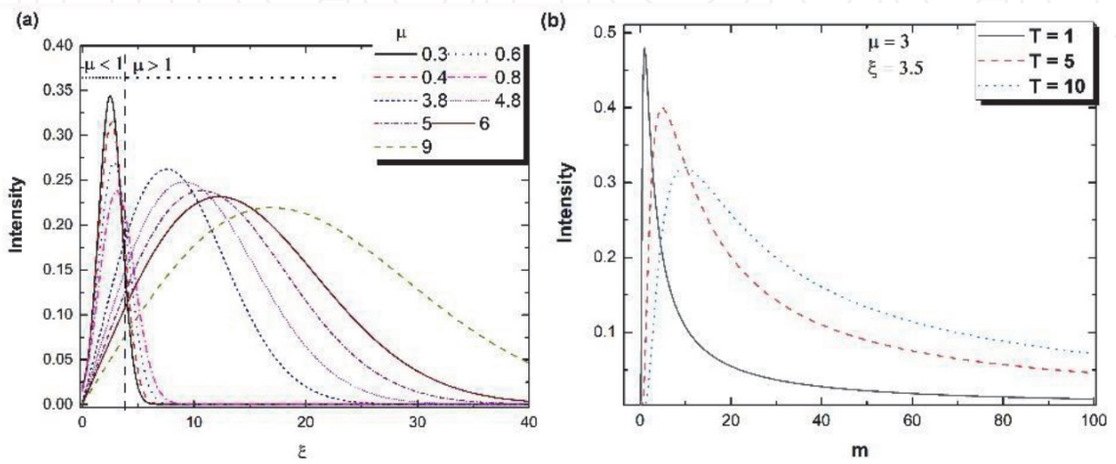


**Figure 4.**
*Spatial dependence of the simulated optical emission of plasma entities with various fractal degrees (a) and mass distribution of the optical emission for various plasma temperature (b).*

strongly heterogenous and it aides particles with an elevated fractalization degree leading to a non-congruent transfer in case of PLD and the lighter elements are predominantly in the outer regions of the plume, while the heavier ones are mainly part of the core.

## 4. A multifractal theoretical approach for understanding the separation of particle flow during pulsed laser deposition of multicomponent alloys

The details of the model have been previously reported in [14]. Let us consider that the evolution of the plasma components (plasma entities) is defined by continuous but non-differential curves, in specific rage of values. This premits us to corelate the properties of plasma plume in a multifractal matrix and thus reducing the dynamics of the individual entities by integrating them with their respective multifractal trajectories (geodesics). Therefore, at extreme times scales with respect to the inverse of the maxim Lyapunov exponent [23], the classical trajectories (deterministic) are replaced by fractal geodesics (families of potential trajectories and the notion of defined spatial coordinates is replaced by that of probability densities.

In such a context, in agreement with the results from [21, 22] at a differentiable resolution scale the ablation plasma dynamics are driven by the specific fractal force:

$$F_F^i = \left[u_F^l + \frac{1}{4}(dt)^{(2/D_F)-1} D^{kl}\partial_k\right]\partial_l u_F^i \tag{8}$$

The introduction of this multifractal force in explicit manner is essential at and is responsible for the structuring of ablation plasma on each component, though a special velocity field. The functionality of our differential system of equations is given by:

$$F_F^i = \left[u_F^l + \frac{1}{4}(dt)^{(2/D_F)-1} D^{kl}\partial_k\right]\partial_l u_F^i = 0 \tag{9}$$

$$\partial_l u_F^l = 0 \tag{10}$$

(9) represents that at a differential scale resolution the multifractal force becomes null, while (10) represents the state density conservation law at non-differentiable scale resolution.

Generally speaking it is rather difficult to obtain an analytic solution for the system of equations considered here, taking into account its multifractal nature (through $u_F^l\partial_l u_F^i$ the multifractal convection and $D^{kl}\partial_l\partial_k u_F^i$ the multifractal type dissipation); also the fractalization type, introduced through multifractal type tensor $D^{kl}$, is left unknown purposefully in this particular representation of the model.

The continuous development of our multifractal model and its implementation for the simulation of *real* plasma like phenomena implies the definition of a three-dimensional plasma like-fluid flow of a with a revolution symmetry around the $z$ axis, and investigate its dynamics through a 2-dimensional projection of the plasma in the (x,$y$) plane.

Considering the symmetry plane ($x$,$y$), the (9) and (10) system becomes:

$$u_{F_x}\frac{\partial u_{F_x}}{\partial x} + u_{Fx}\frac{\partial u_{F_x}}{\partial y} = \frac{1}{4}(dt)^{(2/D_F)-1}\,\mathrm{D}^{yy}\frac{\partial^2 u_{F_x}}{\partial y^2} \tag{11}$$

$$\frac{\partial u_{F_x}}{\partial x} + \frac{\partial u_{F_y}}{\partial y} = 0 \tag{12}$$

Let us solve the equation system (11) and (12) by imposing the following conditions

$$\lim_{y\to 0} u_{F_y}(x,y) = 0,\ \lim_{y\to 0} \frac{\partial u_{F_x}}{\partial y} = 0,\ \lim_{y\to\infty} u_{F_x}(x,y) = 0 \tag{13}$$

$$\Theta = \rho \int_{-\infty}^{+\infty} {u_x}^2 dy = \text{const.}$$

with:

$$D^{yy} = a\exp(i\theta) \tag{14}$$

Let us highlight that existence of a complex phase can be the pathway to a hidden temporal evolution of the system. The variation of a complex phase defines a time-dependence in an implicit manner. This means that for multifractal system can describe both spatial and temporal evolutions. Thus, the choice for $D^{yy}$ gives the possibility of a both spatial and temporal investigations on the LPP plasma dynamics.

The solution of (11) and (12), in their general form in normalized quantities can be written as:

$$X = \frac{x}{x_0}, \mathrm{Y} = \frac{y}{y_0}, \mathrm{U} = u_{F_x}\frac{4y_0^2}{x_o a}, V = u_{F_y}\frac{4y_0^2}{x_o a}, \frac{\left(\frac{\Phi_0}{6\rho}\right)^{1/3}}{\left(a/4\right)^{2/3}} = \frac{x_0^{2/3}}{y_0}, \mu = (\mathrm{dt})^{\left(D_F/2\right)-1} \tag{15}$$

is given according to the method from [21, 22]:

$$U(X,Y) = \frac{3/2}{[\mu X]^{1/3}\exp\left(\frac{i\theta}{3}\right)} \cdot \mathrm{sech}^2\left\{\frac{1/2 Y}{[\mu X]^{2/3}\exp\left(\frac{2i\theta}{3}\right)}\right\} \tag{16}$$

$$V(X,Y) = \frac{(9/2)^{2/3}}{[\mu X]^{1/3}\exp\left(\frac{i\theta}{3}\right)}\left\{\left[\frac{Y}{\mu X^{2/3}\exp\left(\frac{2i\theta}{3}\right)}\right] \cdot \mathrm{sec}\,h^2\left[\frac{1/2 Y}{[\mu X]^{2/3}\exp\left(\frac{2i\theta}{3}\right)}\right] - \tanh\left[\frac{1/2 Y}{[\mu X]^{2/3}\exp\left(\frac{2i\theta}{3}\right)}\right]\right\} \tag{17}$$

To verify the validity of such unusual approach we obtained 3D (**Figure 5**) representations of the transient plasma flow developed based on the solution given by our multifractal system of equations. The transient plasma is *generated* in the framework of our multifractal model as a mixture of various particles with different physical properties (electron, ions, atoms, nanopatricles). This implies that the some multifractal parameters such as the complex phase, fractal dimension or specific length ($x_0$, $y_0$) will include within their values the properties of each individual component. In **Figure 5** we represented the angular separation of the plasma low for different values of the complex phase leading to the appearance of preferential *expansion directions for various elements of the plasma* for $\Theta > 1.5$.

In **Figure 6** we have represented the 2D distribution portraying various plasma flow scenarios with respect to the structure of the laser ablation plasma, starting form a pure, single ionized plasma (only atoms, ions and electrons) towards a multi-component flow (including nanoparticles, molecules or clusters). There is a separation into multiple structures in the two expansion directions (across $X$ and $Y$).

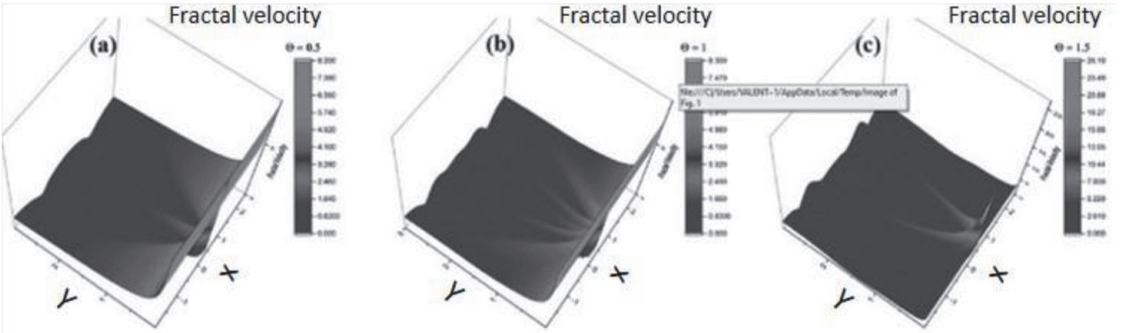


**Figure 5.**
*3D representation of the total fractal velocity field of a multi-fractal plasma flow for various complex phases (0.5 – (a) 1 – (b) 1.5 – (c)).*

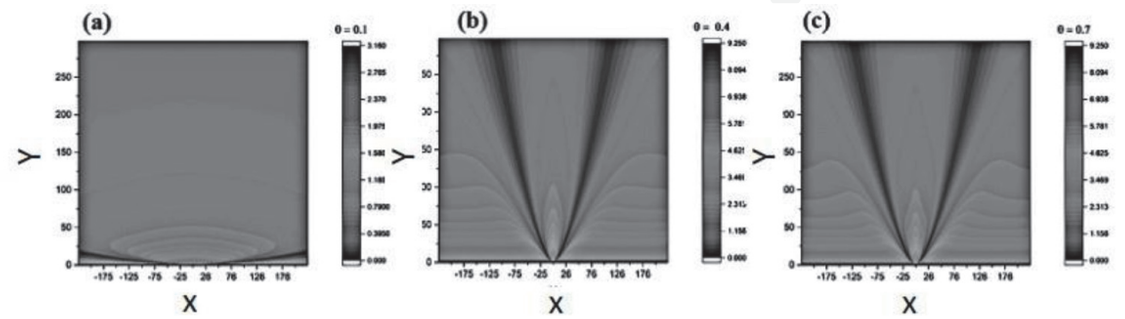


**Figure 6.**
*Total fractal velocity field evolution on the two main directions (X,Y) for a multi fractal system with ξ values of 0.1 (a), 0.4 (b), 0.7 (c).*

For small values of the fractalization degree, which from here on further will be considered as *control* parameter, we define a plasma flow containing only one type of particles thus on plasma component. In **Figure 6(a)**, there can be seen only one plasma structure along the main expansion axis. The increase of this fractalization degree, control parameter, subsequently leads to changes in the homogeneity of the structural units of the plasma (i.e. our model of plasma becomes more heterogeneous in term of plasma particle mass and energy). It is also noticeable the formation of two symmetrically positioned secondary structures (lateral with respect to the main expansion axis). We conclude that those volume of plasma contain mainly components defined by a small physical volume and low kinetic energy. A subsequent increase in the fractalization degree and thus of the heterogeneity of the plasma leads to the formation of lateral-symmetrically situated plasma *structures* each defining different families of particles with physical properties.

An important conclusion extracted from our simulation is that the plasma structuring process is gradual one. For values of $\xi = 0.3 \sim 1$, we can obtain three main lateral structures which are also followed by a continuous internal structuring visible for fractalization degrees $\xi > 1$. Within the framework of our multifractal model this is reversible transition as the distribution often returns to the three-structure system. Another approach of understating this novel phenomenon is to assimilated then with *breathing modes of the fractal system* (oscillatory behavior). The evolution of our plasma model in a multifractal framework attempts a complete transition towards a completely separate flow but the interactions of the multifractal forces between the individual plasma structures are then in charge for the unification of the plasma structures.

The multi-structuring of the laser produced plasma was highlighted by executing cross sections in X direction (see **Figure 7**). In X direction the separation is more obvious first moments of expansion. Each of the new plasma structure is defined by

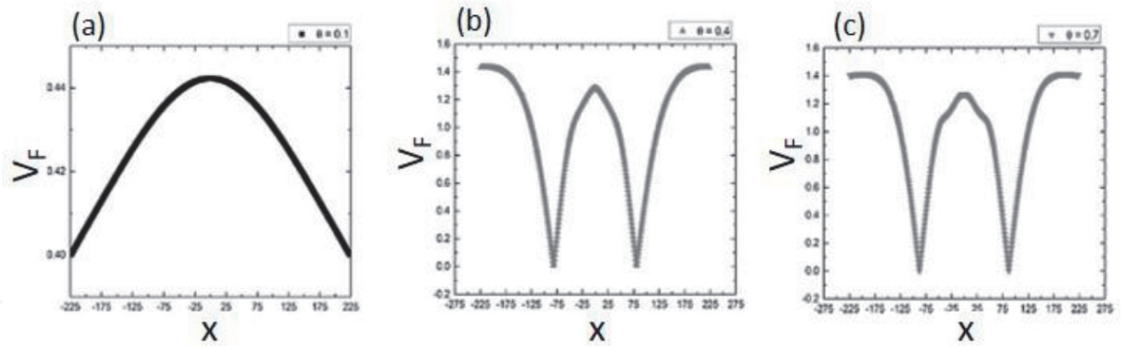


**Figure 7.**
*Transversal cross section for ξ = 0.3 (a), ξ = 1 (b) and ξ = 5 (c).*

different flow velocities as the distance between the maxima of the three structures does not remain constant during expansion. Supplementary investigations were performed by implementing similar data treatment for the Y direction. For the cross section on the Y axis (at X = 0) we can report a more fuzzy separation. This result can be explained as the structuring phenomena of the plasma is not limited to a unique flow axis, being observed in all directions. Moreover, the fractality of the our multifractal system, defined here through ξ and $\mu$, is directly related to the trajectory of the plasma *particles*. As such, for a more complex plasma model (multi-element, multi-structured) the intrinsic dynamic within the plasma structures will induce to a separation on the main expansion axis (at X = 0).

This rather complex multifractal theoretical approach manages to simulate the structuring of a multielement (complex) plasma flow. Nevertheless, this is remains an abstracted view to a real dynamics in various technological application. For the validation of the conceptual and mathematical approach we chose to perfume comparisons with our experimental investigations of laser produced plasmas in quasi-identical conditions to those generally used for pulse laser deposition. Our model is suitable for the description of PLD physical phenomena as in past years various groups have shown [26–29] that in the case of multi-element plasmas there is axial and lateral segregation of the plasma particles during expansion based on their physical properties (mass, melting temperature), which damages the quality and properties of the deposited film.

## 5. Conclusion

The dynamics of a complex multi element plasma was investigated in the framework on a non-differential, multifractal theoretical model. Structuring into multiple plasma fragments were observed for the multi-fractal fluid like system containing structural units with various physical properties. The formation of complex plasma structures during expansion is corelated to the interaction between the transient plasma structural units and it is defined here by the complex phase of the velocity field and the fractalization of the particle geodesics. The multifractal system of equations was simplified by analyzing only two main directions. The plasma splits in multiple structures symmetrically to the main expansion axis.

The multifractal theoretical model was compared with empirical investigations of transient plasmas generated by laser ablation of a multielement metallic targets. The expansion of the plasma plume was monitored by means of ICCD fast camera photography and optical emission spectroscopy. The ICCD fast camera imaging showcased the formation of two or three main plasma structures in the main expansion direction, coupled with a similar phenomenon in the transversal

direction. This complex behavior affects the angular plasma expansion and subsequently affect the spatial distribution of the deposited film. The heterogeneity of the plasma plume velocity field is in good agreement with the theoretical assumption presented in the framework of the non-differential model.

ICCD imaging revealed the splitting of the laser produced plasmas into two different structures, expanding with different velocities. An angular distribution of the front velocity was reconstructed for each of the two plasmas. The specie velocities were correlated to the properties of the elements found in the target (mass and conductivity).

A novel theoretical approach based on multifractal physics was used to simulate the behavior of multi element plasmas. The model considers the relation between the scattering probability, collision frequency and the fractality degree of the plasmas. The angular distribution of the ejected particles was discussed with respect to the fractality of the system. The simulation results are in good agreement with the experimental data.

## Acknowledgements

This work was supported by Romanian Ministry of Education and Research, Nucleu Program LAPLAS VI – contract n. 16 N/2019 and contract n. PD-145/2020.

## Conflict of interest

The authors declare no conflict of interest.

IntechOpen

IntechOpen

## Author details

Stefan Andrei Irimiciuc[1*], Norina Forna[2], Andrei Agop[3], Maricel Agop[4], Stefan Toma[3] and Doriana Forna Agop[2]

1 National Institute for Laser, Plasma and Radiation Physics, 409 Atomistilor Street, 077125 Bucharest, Romania

2 "Gr.T.Popa" University of Medicine and Pharmacy – Iaşi,Str. Universității no. 16, 700115, Iaşi, Romania

3 Material Science and Engineering Department, "Gheorghe Asachi" Technical University of Iasi Romania, 700050, Iasi, Romania

4 Department of Physics, "Gh. Asachi" Technical University of Iasi, 700050, Iasi, Romania

*Address all correspondence to: stefan.irimiciuc@inflpr.ro

IntechOpen

© 2020 The Author(s). Licensee IntechOpen. This chapter is distributed under the terms of the Creative Commons Attribution License (http://creativecommons.org/licenses/by/3.0), which permits unrestricted use, distribution, and reproduction in any medium, provided the original work is properly cited. CC BY

## References

[1] Ojeda-G-P, A., Schneider C.W., Döbeli M., Lippert T., Wokaun A. 2017. Plasma plume dynamics, rebound, and recoating of the ablation target in pulsed laser deposition. Journal of Applied Physics 121 (13): 135306.

[2] Vitiello, M., Amoruso S., Altucci C., de Lisio C., Wang X. 2005. The emission of atoms and nanoparticles during femtosecond laser ablation of gold. Applied Surface Science 248 (1–4): 163–166.

[3] Santos A., Lopes Barsanelli P., Pereira F. M. V., and Pereira-Filho E. R. 2017. Calibration strategies for the direct determination of Ca, K, and Mg in commercial samples of powdered Milk and solid dietary supplements using laser-induced breakdown spectroscopy (LIBS). Food Res. Intern. 94: 72–78.

[4] Diwakar, P. K., Harilal S. S., Hassanein A., Phillips M. C. 2014. Expansion dynamics of ultrafast laser produced plasmas in the presence of ambient argon. Journal of Applied Physics 116 (13): 133301.

[5] Zhou, L. 2017. Two-fluid turbulence modeling of swirling gas-particle flows — A review. Powder Tech. 314: 253–263.

[6] Qiu, Y., Deng B., Kim C. N. 2012. Numerical study of the flow field and separation efficiency of a divergent cyclone. Powder Techn. 217: 231–237.

[7] Irimiciuc, S. A., Bulai G., Gurlui S., Agop M. 2018. On the separation of particle flow during pulse laser deposition of heterogeneous materials - a multi-fractal approach. Powder Tech. 339: 273–280.

[8] Nedeff, V., Lazar G., Agop M., Eva L., Ochiuz L., Dimitriu D., Vrajitoriu L., C. Popa. 2015. Solid components separation from heterogeneous mixtures through turbulence control. Powder Techn. 284: 170–186.

[9] Nedeff, V., Lazar G., Agop M., Mosnegutu E., Ristea M., Ochiuz L., Eva L., Popa C. 2015. Non-linear Behaviours in complex fluid dynamics via non-differentiability. Separation Control of the Solid Components from Heterogeneous Mixtures. Powder Techn. 269: 452–460.

[10] Kelessidis, V. C., and G. Mpandelis. 2004. Measurements and prediction of terminal velocity of solid spheres falling through stagnant Pseudoplastic liquids. Powder Tech. 147 (1–3): 117–125.

[11] Zhang, S, Kuwabara S., Suzuki T., Kawano Y., Morita K., Fukuda K. 2009. Simulation of solid-fluid mixture flow using moving particle methods. J. Com. Phys. 228 (7): 2552–2565.

[12] Monaghan, J.J. 1992. Smoothed particle hydrodynamics. An. Rev. Astro. Astrophys., 543–74.

[13] Irimiciuc, S., Bulai G., Agop M., Gurlui S. 2018. Influence of laser-produced plasma parameters on the deposition process: In situ space- and time-resolved optical emission spectroscopy and fractal modeling approach. Appl. Phys. A: Mat. Sci. Process. 124(9):615

[14] Irimiciuc, S.A., Gurlui S., Nica P., Focsa C., Agop M. 2017c. A compact non-differential approach for modeling laser ablation plasma dynamics. Journal of Applied Physics 121 (8).

[15] Ngom, B. D., S. Lafane, S. Abdelli-Messaci, T. Kerdja, and M. Maaza. 2016. Laser-produced Sm1−xNdxNiO3 plasma dynamic through Langmuir probe and ICCD imaging combined analysis. Appl. Phys. A: Mat. Sci. Proces. 122 (1): 1–7.

[16] Singh, J., R. Kumar, Awasthi S., Singh V., Rai A. K. 2017. Laser induced breakdown spectroscopy: A rapid tool for the identification and quantification of minerals in cucurbit seeds. Food Chemistry 221: 1778–1783.

[17] Irimiciuc, S. A., Mihaila I., Agop M. 2014. Experimental and theoretical aspects of a laser produced plasma. Physics of Plasmas 21: 093509.

[18] Anoop, K. K., Polek M. P., Bruzzese R., Amoruso S., Harilal S. S. 2015. Multidiagnostic analysis of ion dynamics in ultrafast laser ablation of metals over a large Fluence range. Journal of Applied Physics 117 (8).

[19] Geohegan, D. B. 1992. Fast-Iccd photography and gated photon counting measurements of blackbody emission from particulates generated in the KrF-laser ablation of BN and YBCO. MRS Proceedings 285 (January): 27.

[20] Geohegan, D. B., Puretzky A. A., Duscher G., Pennycook S. J. 1998. Time-resolved imaging of gas phase nanoparticle synthesis by laser ablation. Applied Physics Letters 72 (23): 2987–2989.

[21] Merches, I., Agop M.. 2015. Differentiability and Fractality in Dynamics of Physical Systems. World Scientific.

[22] Agop M., Merches I. 2019, Operational Procedures Describing Physical Systems, CRC Press, Florida.

[23] Cristescu, C.P. (2008).Non-linear Dynamics and Chaos : Theoretical Fundaments and Applications. Bucharest: Romanian Academy Publishing House.

[24] Mandelbrot, B. (2006).The Fractal Geometry of Nature. New York: W.H. Freeman And Company.

[25] Nottale, L. (2011).Scale Relativity and Fractal Space-Time : A New Approach to Unifying Relativity and Quantum Mechanics. London: Imperial College Press.

[26] Canulescu, S., E. L. Papadopoulou, D. Anglos, Th. Lippert, C. W. Schneider, and A. Wokaun. 2009b. Mechanisms of the laser plume expansion during the ablation of LiMn2O4. J.Applied Physics 105 (6): 063107.

[27] Canulescu, St., Döbeli M., Yao X., Lippert T., Amoruso S., Schou J. 2017. Nonstoichiometric transfer during laser ablation of metal alloys. Phys. Rev. Mat. 1 (7): 073402.

[28] Sloyan, Katherine a., Timothy C. May-Smith, Robert W. Eason, and James G. Lunney. 2009. The effect of relative plasma plume delay on the properties of complex oxide films grown by multi-laser, multi-target combinatorial pulsed laser deposition. Appl. Surf. Sci. 255 (22): 9066–9070

[29] O'Mahony, D, Lunney J., Dumont T., Canulescu S., Lippert T., Wokaun A. 2007. Laser-produced plasma ion characteristics in laser ablation of Lithium Manganate. Appl. Surf. Sci. Science 254 (4): 811–815.